

See discussions, stats, and author profiles for this publication at: <https://www.researchgate.net/publication/242012760>

Mathematical Modelling of Insect--Like Flapping Wings for Application to MAVs

Article · January 2009

CITATIONS

0

READS

925

3 authors:



A. Roshanbin

Université Libre de Bruxelles

17 PUBLICATIONS 182 CITATIONS

[SEE PROFILE](#)



C. Collette

Université Libre de Bruxelles

207 PUBLICATIONS 48,872 CITATIONS

[SEE PROFILE](#)



A. Preumont

Université Libre de Bruxelles

314 PUBLICATIONS 6,853 CITATIONS

[SEE PROFILE](#)

Some of the authors of this publication are also working on these related projects:



Vehicle Dynamics and Control [View project](#)



Design of Hummingbird-like Flapping Wing MAV [View project](#)

Mathematical Modelling of Insect–Like Flapping Wings for Application to MAVs

A. Roshanbin

Department of Mechanical Engineering and Robotics, University of Brussels av. F.D.Roosevelt 50,
1050 Brussels - Belgium

Email: ali.roshanbin@ulb.ac.be

C. Collette

Department of Mechanical Engineering and Robotics, University of Brussels av. F.D.Roosevelt 50,
1050 Brussels – Belgium

Email: ccollett@ulb.ac.be

A. Preumont

Department of Mechanical Engineering and Robotics, University of Brussels av. F.D.Roosevelt 50,
1050 Brussels – Belgium

Email: apreumon@ulb.ac.be

Abstract: The flight of birds or insects has fascinated physicists and biologists for many centuries. Flapping motion, as shown by many nature flyers, is the most efficient way of flying objects whose size are smaller than 15 cm. In this paper a mathematical modelling of insect-like flapping wings for application to MAVs is presented. To this aim, the first part of the paper gives a brief review of unsteady aerodynamics for flapping wing flight and the most important physical features of the flow are identified. Then a simulation of comprehensive nonlinear MAV model based on quasi-steady method is developed. This model enables us to investigate the influence of each parameter change in flight force generation.

Keywords: Insect flight, flapping wing, aerodynamics, micro aerial vehicle.

Micro aerial vehicles (MAVs) have received a great deal of attention in the past decade due to various types of surveillance applications including rescue, hazardous environment exploration, sensor deployment, planetary exploration etc. Even though these MAV developments are impressive, the field of flapping wing micro air vehicles is still in its infancy. Each one of these designs is unique and utilizes a specific aerodynamic principle. However, at this time, a systematic design philosophy for a range of flapping wing micro air vehicles is lacking.

Flapping wing vehicles offer a number of advantages over fixed and rotary wing vehicles. Fixed wing vehicles, for example, do not have the required agility necessary for obstacle-avoidance in indoor flight and are incapable of hovering. Although rotary wing vehicles offer hovering capability, they suffer from wall-proximity effects and are too noisy and inefficient (particularly at small scale) [1]. Since power on a small flying platform is in limited supply, this is a very important constraint. Hence, flapping wing flying machines are more suitable for micro air vehicle missions involving reconnaissance and surveillance, especially in confined areas.

There are two classes of aerial flapping flight: bird-like and insect-like. Birds have an endoskeleton so that muscles attached to bones along the wing are used for flight and manoeuvring. This, however, makes them heavy and relatively less efficient (in terms of

specific power). They can compensate for this by spending a significant time of their flight gliding. Birds consequently spend most of their time in forward flight and are, therefore, too fast to be useful for indoor applications. Insects, on the other hand, possess an exoskeleton: all actuation is carried out at the wing root and, consequently, the wing structure is very light, generally accounting for ~1% of the insect's weight [2]. This makes insect flight very attractive as a model, while also satisfying all the other requirements of the flight identified above (especially hover) for an indoor MAV.

Through a cycle, the motion of the flapping wing can be divided broadly into translational motion, called the flapping, and rotational motion, called feathering. The translational phase consists of two half-strokes: the downstroke and the upstroke. The downstroke refers to the motion of the wing from its rearmost position (relative to the body) to its foremost position. The upstroke describes the return cycle. At either ends of the half-strokes, the rotational phases come into play, whereby the wing rotates rapidly and reverses direction for the subsequent half-stroke. *Supination* and *pronation* are the terms used to describe the wing rotation at the end of downstroke and upstroke, respectively. The wings flap back and forth about a plane called the stroke plane. In normal hovering flight, most insects use horizontal stroke plane and in forward flight they use inclined stroke plane (Fig. 1).

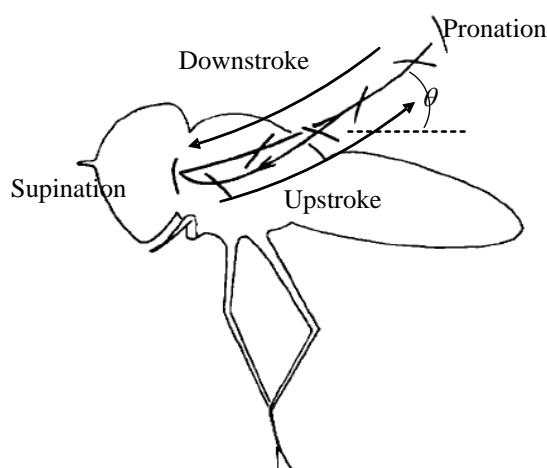


Fig 1: Insect flapping with inclined stroke plane [2]

I. INSECT FLIGHT AERODYNAMICS

The flow associated with insect flapping flight is incompressible, laminar and unsteady, and occurs at low Reynolds numbers (for large insects, Re lies between 5000 and 10000, but it approaches 10 for the smallest ones) [3], [16]. Despite their short stroke lengths, insect wings can generate forces much higher than their quasi-steady equivalents due to the presence of a number of unsteady and vertical aerodynamic effects. In fact, At first glance, their flight seems improbable using standard aerodynamic theory. This section attempts to cover four main relevant aerodynamic phenomena:

1. Rotational circulation
2. Wake capture
3. Clap and fling
4. Leading-edge vortex

It should be noted that these models are appropriate in low advance ratio situations (the ratio of flight speed to the speed of wing tip), which occur whenever natural fliers are not gliding or soaring.

1) Rotational circulation

Dickinson [4] has extensively studied the effect of wing rotation during the transition from downstroke to upstroke in a mechanical model of the *Drosophila melanogaster* wing. This study has revealed that mechanism of rotational circulation (Kramer effect) is similar to the *Magnus effect*. Therefore, the timing of supination relative to stroke reversal is critical in determining the magnitude of the forces produced. Large positive forces are generated when supination precedes stroke reversal, whereas negative forces are registered if supination is delayed. By asymmetrically varying force production in this way, flies could readily produce turning moments for control.

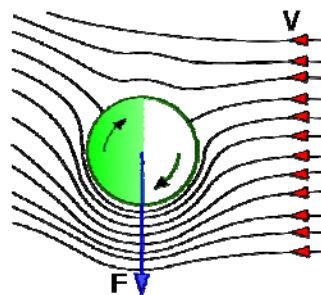


Fig 2: Magnus effect [5]

2) Wake capture

As the wing reverses stroke it sheds both the leading and the trailing edge vortices. These shed vortices induce a strong inter vortex velocity field. As the wing reverses direction, it encounters the enhanced velocity and acceleration fields, thus resulting in higher aerodynamic forces immediately following stroke reversal. In other words, the wake behind a flying object contains energy imparted to the surrounding fluid in the form of momentum. Wing passage through the wake could, therefore, be a method to recover some of this lost energy and utilise it usefully for flight. The importance of wake capture was also suggested by Grodnitsky and Morozov [6] who proposed that insects and birds have special mechanisms whereby they extract energy back from their near vortex wake.

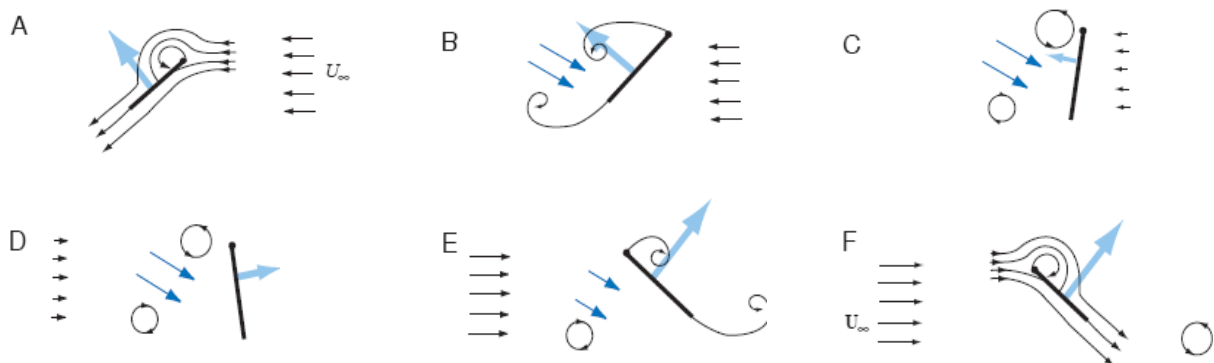


Fig 3: wake capture mechanism [7]

3) Clap and fling

One of the unsteady mechanisms is known as the “clap and fling” mechanism, proposed by Weis-Fogh [8] based on observation of the small wasp *Encarsia formosa* hovering. Some other small insects, for example, fruitfly *Drosophila virilis*, have also been observed employing the clap and fling mechanism in some circumstances [8]. Fig.4. depicts the wing kinematics and the consequent vortex development. The wing surfaces press together at the end of the upstroke for an extended period of time, mimicking a motion much like two hands coming together for a “clap”. As the wings separate and open for the next downstroke, they rotate around their trailing edges. The trailing edges remain adjacent and connected together until the leading edges fling apart. At this instant, the wings form a V shape before they begin parting away from each other. The sudden translation of opposing section causes air to rush into the widening gap and produce high strength vortices of equal and opposite sign. This leads to large circulation and lift on the wing. Because of the symmetry of the motion, the magnitudes of the two circulations about the two wings are equal and the senses are opposite. One wing with its circulation acts like the starting vortex of the other wing and vice versa, then no starting vortices need to be shed as the wings move apart. Weis-Fogh argued that this absence of starting vortices avoids the delay in the build up of the maximum lift force required by the Wagner effect and brings a high overall lift over the wingbeat cycle.

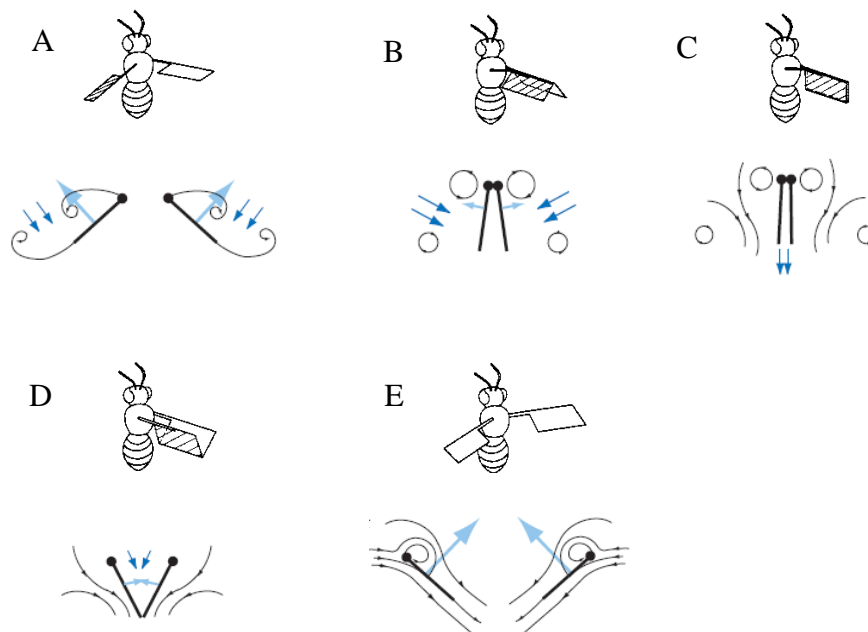


Fig 4: Weis-Fogh clap and fling mechanism [8], [7]

4) Leading-edge vortex

Although a number of unsteady aerodynamic phenomena pertaining to insect-like flapping flight have been identified above, they are still unable to explain the high lift required to sustain flight. This remained a mystery essentially until 1996 when Ellington and his co-workers discovered the delayed stall and leading edge vortex (LEV) [9].

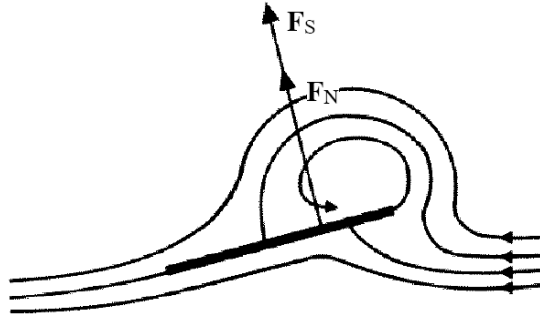


Fig 5: The generation of leading edge suction [10]

Insects fly at high angle of attack, and through their motion, a leading edge vortex and a trailing edge vortex develop on the wing. However, contrary to a translating 2D airfoil or plate, the LEV of the wing remains constant in shape and size. The reason is that the flow is fully three-dimensional; a strong spanwise flow exists that stabilizes the vortex (Fig.6.). This spanwise flow convects the vorticity out toward the wing tip, and removes energy from it, and hence, limits its growth and shedding. This prolonged attachment of the leading edge vortex produces suction force, F_s , normal to the plane of the wing and therefore sums with the normal force, F_N (Fig.5.).

LEVs have been seen on the wings of both large insects and small ones [10]. Liu et al. found that because of the presence of the LEV, the wings of a hovering hawkmoth were able to generate vertical forces up to about 40% greater than required to support its weight [11]. The LEV is, therefore, fundamental in explaining the large forces generated by insect-like flapping wings.

II. AERODYNAMIC MODELING

Conventional fixed and rotary wing aircrafts are designed on the basis of steady state aerodynamics in which the flow over the wings generates constant lift and drag forces. On the other hand, for flapping wing insects, the lift and drag forces change sharply over one complete cycle of flapping motion. One approach that is often used is to calculate the average lift over a flapping cycle. Here, wing flapping is approximated by a series of steady-state flow conditions over the wing sections. This method is also termed quasi-steady blade element analysis which is employed in this study.

According to the aerodynamic phenomena mentioned in the previous section, a flapping wing at small Reynolds numbers experiences four different instantaneous forces all acting normal to the wing surface:

$$F_{inst} = F_{tr} + F_{rot} + F_{wc} + F_{c\&f} \quad (1)$$

where F_{inst} is the instantaneous aerodynamic force on the wing, F_{tr} is the instantaneous force due to translational force, F_{rot} is the rotational force, F_{wc} is the wake capture force and $F_{c\&f}$ is the force due to the clap and fling phenomena.

Since wake capture and clap and fling force are rather hard to approximate analytically they are omitted from the dynamical model. Therefore, it should be noted that the obtained results

are underestimates. The components of normal, $F_{tr,N}$, and tangential, $F_{tr,T}$, translational force based on the standard formula for airfoils are calculated as [10]:

$$\begin{aligned} F_{tr,T} &= \frac{1}{2} \rho A_w C_T U_{cp}^2 \\ F_{tr,N} &= \frac{1}{2} \rho A_w C_N U_{cp}^2 \end{aligned} \quad (2)$$

Where, U_{cp} is the velocity of the wing at the center of pressure. In small advance ratio, this parameter can be defined as:

$$U_{cp}^2 = \hat{r}_2 L \dot{\phi} \quad (3)$$

In which \hat{r}_2 is the normalized distance of center of pressure from wing base:

$$\hat{r}_2^2 = \frac{\int_0^L c r^2 dr}{L^2 A_w} \quad (4)$$

Where, A_w denotes the wing area, ρ the density of air, L the wing length, $\dot{\phi}$ stroke velocity, and c wing chord width. The force coefficients, C_N , C_T , for the model wing were measured in [4] and fitted with the following equations:

$$\begin{aligned} C_N &= 3.4 \sin \alpha_1 \\ C_T &= \begin{cases} 0.4 \cos^2(2\alpha_1) & 0 \leq \alpha_1 \leq 45^\circ \\ 0 & otherwise \end{cases} \end{aligned} \quad (5)$$

α_1 stands for the angle of attack. A quasi-steady treatment of the aerodynamic force due to wing rotation, $F_{rot,N}$, was derived by Fung and is calculated by [13]:

$$F_{rot,N} = \frac{1}{2} \rho A_w C_{rot} \hat{c} c_m \dot{\alpha}_1 U_{cp} \quad (6)$$

Where c_m is the maximum wing chord width, and the theoretical value of rotational coefficient, C_{rot} , is given by [13]:

$$C_{rot} = 2\pi(0.75 - \hat{x}_0) \quad (7)$$

And

$$\hat{c} = \frac{\int_0^L c^2 r dr}{\hat{r}_2 L A_w c_m} \quad (8)$$

\hat{x}_0 is the dimensionless distance of the longitudinal rotation axis from the leading edge. Therefore, according to the fig.7. the total lift and drag forces are computed as follows:

$$F_N = F_{ir,N} + F_{rot.N} \quad (9)$$

$$F_T = F_{ir,T} \quad (10)$$

$$F_D = F_N \cos(\alpha_2) + F_T \sin(\alpha_2) \quad (11)$$

$$F_L = F_N \sin(\alpha_2) - F_T \cos(\alpha_2) \quad (12)$$

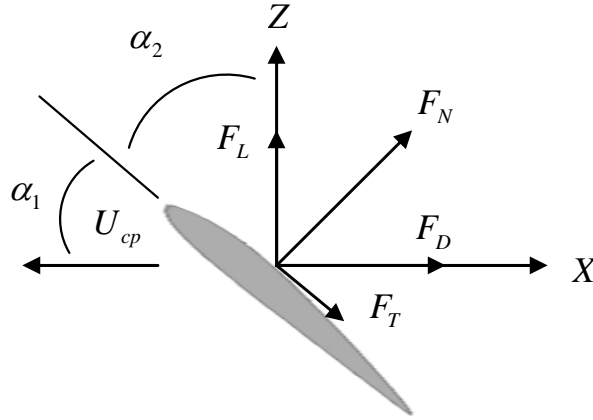


Fig 7: wing kinematic parameters

III. BODY DYNAMICS MODEL

For dynamic modeling we consider the insect as a rigid body of 6 degree of freedom. Therefore, wing inertial is disregarded in this study. As shown in the Fig.8. the coordinate system are fixed to the body at the center of mass, and x, y, z axes are the principal axes. Therefore, the Euler equations have been utilized for modeling the rotation. The equation of motion can be governed by:

$$\begin{aligned} M\dot{v}_1 + M(\omega_2 v_3 - \omega_3 v_2) &= F_1 \\ M\dot{v}_2 + M(\omega_3 v_1 - \omega_1 v_3) &= F_2 \\ M\dot{v}_3 + M(\omega_1 v_2 - \omega_2 v_1) &= F_3 \end{aligned} \quad (13)$$

$$\begin{aligned} I_1 \dot{\omega}_1 - (I_2 - I_3) \omega_2 \omega_3 &= T_1 \\ I_2 \dot{\omega}_2 - (I_3 - I_1) \omega_3 \omega_1 &= T_2 \\ I_3 \dot{\omega}_3 - (I_1 - I_2) \omega_1 \omega_2 &= T_3 \end{aligned} \quad (14)$$

I_i , $i=1,2,3$ are the body moments of inertia, T_i , $i=1,2,3$ are torques and F_i , $i=1,2,3$ are force acting on the body. For representing the spatial position and orientation of the insect, the set of equation (13) and (14) should be transformed to the reference frame. One of the best-known transformations is the Euler angles. Then, the linear velocity in fixed frame is:

$$V_{ref} = Rv \quad (15)$$

In which R is the rotation matrix of the body frame relative to the reference frame.

The vector of rotational velocities on the body fixed coordinate system in terms of the Euler angles (φ, θ, ψ) is [14]:

$$\begin{aligned} \vec{\omega} = & (\dot{\varphi} \sin \theta \sin \psi + \dot{\theta} \cos \psi) \hat{i} + \\ & (\dot{\varphi} \sin \theta \cos \psi - \dot{\theta} \sin \psi) \hat{j} + (\dot{\varphi} \cos \theta + \dot{\psi}) \hat{k} \end{aligned} \quad (16)$$

And rotational acceleration is:

$$\begin{aligned} \dot{\vec{\omega}} = & (\ddot{\varphi} \sin \theta \sin \psi + \dot{\theta} \dot{\varphi} \cos \theta \sin \psi + \\ & \dot{\psi} \dot{\varphi} \sin \theta \cos \psi + \ddot{\theta} \cos \psi - \dot{\psi} \dot{\theta} \sin \psi) \hat{i} + \\ & (\ddot{\varphi} \sin \theta \cos \psi + \dot{\theta} \dot{\varphi} \cos \theta \cos \psi - \\ & \dot{\psi} \dot{\varphi} \sin \theta \sin \psi - \ddot{\theta} \sin \psi - \dot{\psi} \dot{\theta} \cos \psi) \hat{j} + \\ & (\ddot{\varphi} \cos \theta - \dot{\theta} \dot{\varphi} \sin \theta + \dot{\psi}) \hat{k} \end{aligned} \quad (17)$$

After substituting the equations (16) and (17) into (14) and (15) into (13) with proper simplification the equation of motion in terms of the Euler angles can be reached.

For computing the total forces and moments in the body frame, two steps are needed. First the total forces and moments should be calculated in stroke plane.

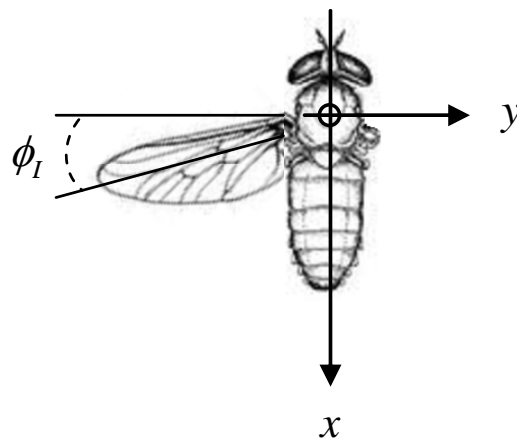


Fig 8: Definition of fixed-body axis and wing flapping angle

$$\vec{F}_{Stroke\ plane}^l = F_D^l \cos \phi_l \hat{i} + F_D^l \sin \phi_l \hat{j} + F_L^l \hat{k} \quad (18)$$

$$\vec{F}_{Stroke\ plane}^r = F_D^r \cos \phi_r \hat{i} - F_D^r \sin \phi_r \hat{j} + F_L^r \hat{k} \quad (19)$$

Therefore

$$\vec{F}_{Stroke\ plane} = \vec{F}^r + \vec{F}^l \quad (20)$$

$$\begin{aligned} \vec{T}_{Stroke\ plane} &= \hat{r}_2 L(\sin \phi_r \hat{i} + \cos \phi_r \hat{j}) \times \vec{F}^r + \\ &\hat{r}_2 L(\sin \phi_l \hat{i} + \cos \phi_l \hat{j}) \times \vec{F}^l \end{aligned} \quad (21)$$

Then a transformation from stroke plane to body frame should be done.

$$\begin{Bmatrix} \vec{F} \\ \vec{T} \end{Bmatrix} = \begin{bmatrix} R_{bs} & R^T & 0 \\ -R_{bs} p_{bs} & 0 & R_{bs} \end{bmatrix} \begin{Bmatrix} \vec{F}_{Stroke\ plane} \\ F_G \\ \vec{T}_{Stroke\ plane} \end{Bmatrix} \quad (22)$$

In which F_G represents the gravitational force, p_{bs} is the translational matrix of the origin of the body frame from the stroke plane, and R_{bs} is the rotation matrix of the body frame relative to the stroke plane.

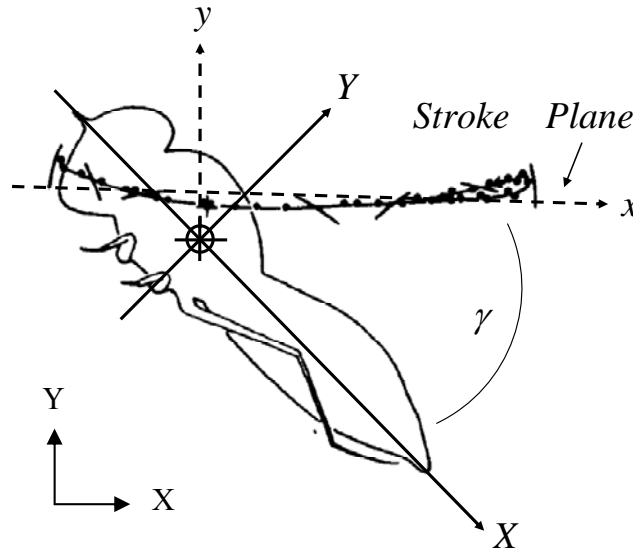


Fig 9: Definition of body frame and stroke plane frame [15]

IV. SIMULATION RESULTS

In order to investigate the modelling and effectiveness of rotational circulation on total flight forces, computer simulations for the open-loop system are conducted. A 6DOF nonlinear MAV model is used for this purpose. The simulation model incorporates yaw, pitch, and body roll motions, as well as position of mass center. Quasi-steady method is used to estimate the aerodynamic flight forces. This software is at the early stage of development. The MAV parameters are given in Table 1. These parameters are not realistic.

TABLE. 1

MAV Parameters

Parameter	Value	Unit
M	0.003163	kg
I_1	$3e-8$	$kg.m^2$
I_2	$1.9e-6$	$kg.m^2$
I_3	$1.9e-6$	$kg.m^2$
L	0.045	m
A_w	$5.0625e-004$	m^2
ρ	1.2	kg / m^3
\hat{x}_0	0.25	-
\hat{r}_2	0.65	-
\hat{C}	0.6	-
c_m	0.01	m

Simulations involve a symmetrical flapping with the frequency of 50 Hz and 50 deg stroke amplitude. The active wing rotation has been chosen as a feathering mechanism. The MAV runs at an initial linear and angular velocity of zero with the horizontal stroke plane.

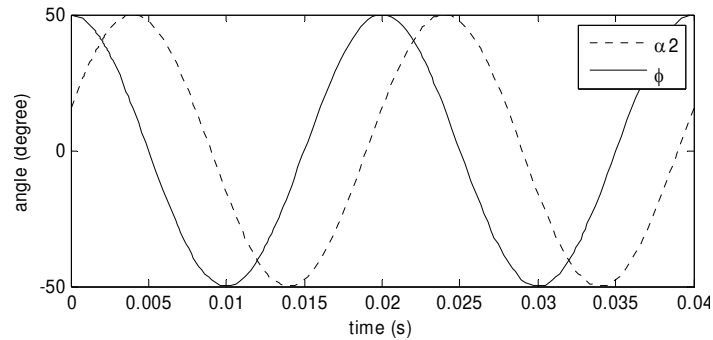


Fig. 10. Stroke and rotation angles in the case of advanced wing rotation

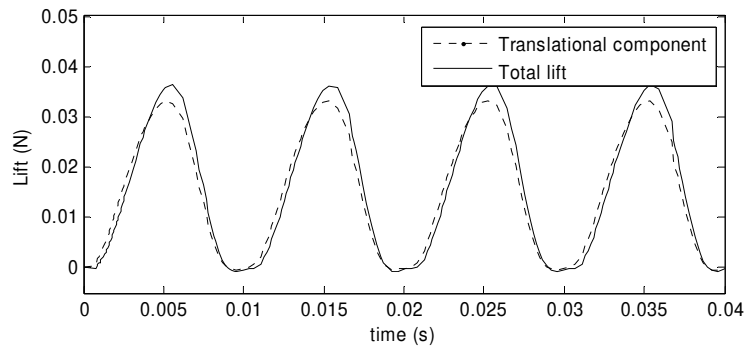


Fig. 11. Time history of the lift force in body frame, advanced wing rotation

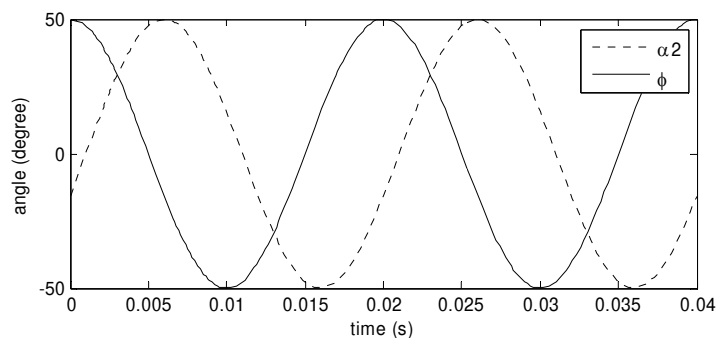


Fig. 12. Stroke and rotation angles in the case of delayed wing rotation

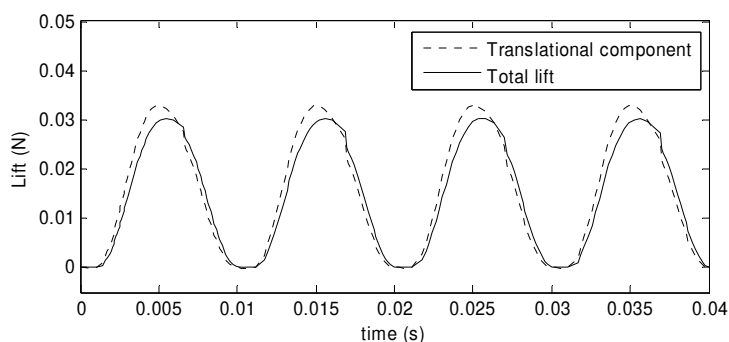


Fig. 13. Time history of the lift force in body frame, delayed wing rotation

Comparison of the wing rotation phases relative to translation motion is shown in Fig. 10 to 16. s we can see, an advance in rotation results in a positive lift peak, whereas a delay in rotation results in negative lift. Also for the symmetrical rotation the wing rotation dose not have a significant contribution in lift force generation (Fig.16). These results are consistent with experimental data that has been provided by Dickinson [4].

Fig.17. to 20 show the simulation results using the lift and drag forces with symmetrical wing rotation (fig.16). Due to the time-varying behaviour of aerodynamic forces for insect flight, the dynamics of the insect shows an oscillatory motion. The simulation concept has been demonstrated in Fig.14.

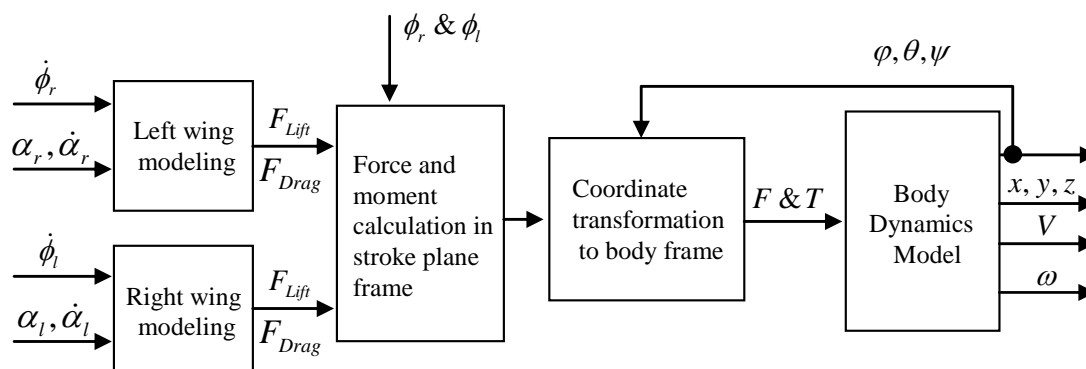


Fig. 14. Block diagram structure of modelling

V. CONCLUSION

In this paper, a mathematical modelling of insect-like flapping wings for application to MAVs was presented. A nonlinear MAV model, with six degrees of freedom, incorporating quasi-steady method to estimate the aerodynamic flight forces was used for simulation purpose.

The effectiveness of timing of wing rotation was investigated through digital simulations. The results were consistent with the experimental data that has been provided by Dickinson. Finally, it is necessary to account the wing inertia to simulate the insect with the passive wing rotation since the above model was based on active wing rotation and the wing inertia was neglected. This paper is the first step of an effort to understand and mimic the motion of insect and small birds and the software is at the early stage of development.

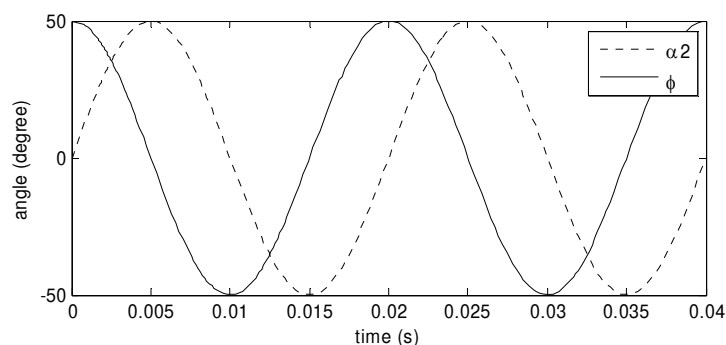


Fig. 15. Stroke and rotation angles in the case of symmetrical wing rotation

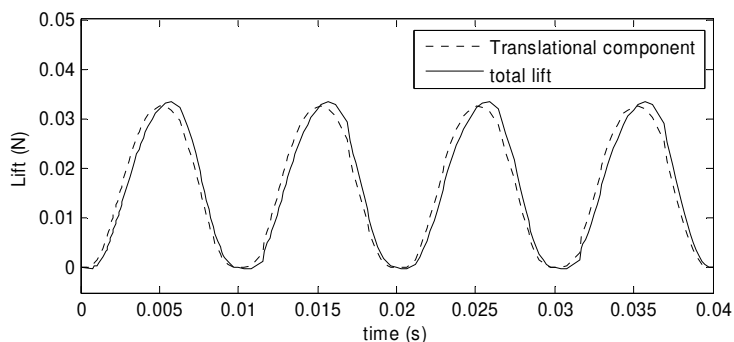


Fig. 16. Time history of the lift force in body frame, symmetrical wing rotation

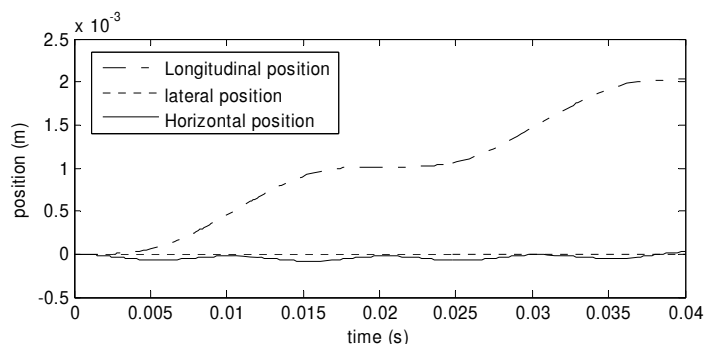


Fig. 17. Position simulation results in the case of symmetrical wing rotation

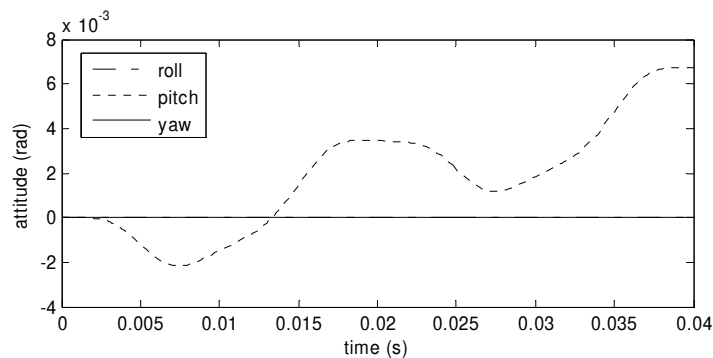


Fig. 18. Attitude simulation results in the case of symmetrical wing rotation

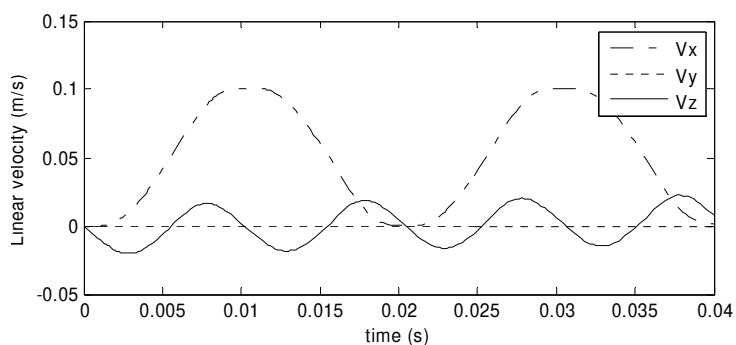


Fig. 19. Time history of linear velocity in the case of symmetrical wing rotation

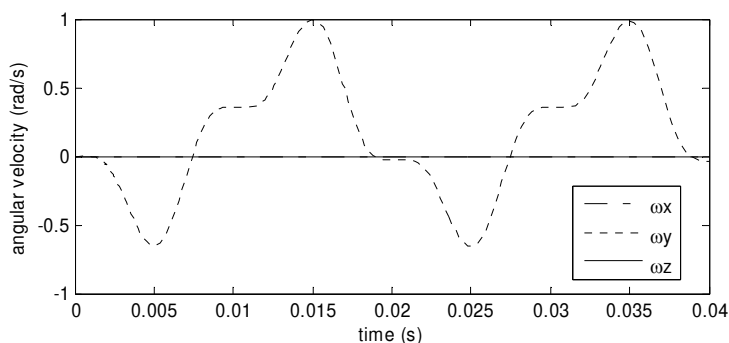


Fig. 20. Time history of angular velocity in the case of symmetrical wing rotation

REFERENCES

- [1] Woods MI., Henderson JF., Lock GD., 'Energy requirements for the flight of micro air vehicles' *Aeronaut J*, Vol. 105, paper No. 2546, pp. 135–49, 2001.
- [2] Ellington CP., 'The aerodynamics of hovering insect flight: II. Morphological parameters' *Philos Trans R Soc London Ser B*, Vol. 305, pp. 17–40, 1984.
- [3] Ansari S. A., Zbikowski R., Knowles K., 'Aerodynamics Modelling of Insect-Like Flapping Flight for Micro Air Vehicles', *Progress in Aerospace Sciences*, Vol. 42, pp. 129-172, 2006.
- [4] Dickinson M. H., Lehmann Fritz-Olaf, Sane S. P., 'Wing Rotation and the Aerodynamic Basis of Insect Flight', *Science*, Vol. 284, pp. 1954-1960, 1999.
- [5] http://en.wikipedia.org/wiki/Magnus_effect.
- [6] Grodnitsky DL., Morozov PP., 'Vortex formation during tethered flight of functionally and morphologically twowinged insects, including evolutionary considerations on insect flight', *J. Exp. Biol.*, Vol. 182, pp. 11–40, 1993.
- [7] Sane S. P., 'The Aerodynamics of Insect Flight', *J. Exp. Biol.*, Vol. 206, pp. 4191-4208, 2003.

- [8] Weis-Fogh T., 'Quick Estimates of Flight Fitness in Hovering Animals, Including Novel Mechanism for Lift Production' *J. Exp. Biol.*, Vol. 59, No. 1, pp. 169–230, 1973.
 - [9] Ellington CP., van den Berg C., Willmott AP., Thomas ALR. 'Leading-edge vortices in insect flight' *Nature*, Vol. 384, pp. 626–30, 1996.
 - [10] Dickinson M. H., and Gotz K. G., 'Unsteady Aerodynamic Performance of Model Wing at Low Reynolds Numbers', *J. Exp. Biol.* Vol. 174, pp. 45-64, 1993.
 - [11] Liu H., Ellington CP., Kawachi K., van den Berg C., Willmott AP. 'A computational fluid dynamic study of hawkmoth hovering' *J. Exp. Biol.*, Vol. 201, pp. 461–77, 1998.
 - [12] <http://images.google.be/imgres?imgurl=http://www.zoo.cam.ac.uk>
 - [13] Sane S. P. and Dickinson M. H., 'The Aerodynamic Effects of Wing Rotation and a Revised Quasi-Steady Model of Flapping Flight', *J. Exp. Biol.* Vol. 205, pp. 1087-1096, 2002.
 - [14] Rosenberg R., *Analytical Dynamics of Discrete Systems*, (Plenum Press, New York, 1977).
 - [15] Ellington C. P., 'The Aerodynamics of Hovering Insect Flight. III Kinematics', *Phil. Trans. R. Soc. Lond. B*, Vol. 305, pp. 41-78, 1984.
- Ellington C. P., 'The Novel Aerodynamics of Insect Flight: Application to Micro-Air Vehicles', *J. Exp. Biol.* Vol. 202, pp. 3439-3448, 1999.